

# Solubilization of hydrophobic molecules in nanoparticles formed by polymer–surfactant interactions

Gilat Nizri, Shlomo Magdassi \*

*Casali Institute of Applied Chemistry, Institute of Chemistry, The Hebrew University of Jerusalem, Jerusalem 91904, Israel*

Received 16 February 2005; accepted 29 April 2005

Available online 21 June 2005

## Abstract

The interaction between the anionic surfactant, sodium dodecyl sulfate, and the polyelectrolyte, poly(diallyldimethylammonium chloride), may lead to formation of nanoparticles dispersed in water. The morphology of the resulting nanoparticles and their ability to solubilize hydrophobic molecules were evaluated. As shown by SEM and AFM imaging, the particles are spherical, having a diameter of about 20 nm. The solubilization within the nanoparticles was tested with pyrene, a fluorescence probe, and Nile Red, a solvatochromic probe. It was found that for Nile Red the solubilization within the nanoparticles is at lower polarity than for SDS micelles, and from pyrene solubilization it appears that the hydrophobicity of the nanoparticles depends on the ratio between the SDS molecules and the charge unit of the polymer.

© 2005 Elsevier Inc. All rights reserved.

**Keywords:** SDS; PDAC; Surfactant; Polymer; Nanoparticles; Solubilization; Pyrene; Nile Red; CAC; CMC

## 1. Introduction

Polymer–surfactant interaction in aqueous solutions has been intensively studied [1–8], due to the growing applications of these systems in various fields, such as detergents, hair care products, foams, emulsions, mineral recovery, and DNA transfections.

So far, most of these interactions have been elaborated in systems containing nonionic polymers and ionic surfactants. The surfactant in these systems is weakly bound to the polymer chains, whether as a single molecule or as an aggregate.

Interactions between a charged polymer and an oppositely charged surfactant usually result in phase separation owing to strong electrostatic forces. These forces may induce precipitation of a polymer–surfactant complex at certain surfactant concentration range. However, as reported by Dubin and Oteri [9] for systems containing PDAC, SDS, and a nonionic surfactant (Triton X-100), aggregation could occur without accompanying precipitation at specific ranges

of the ionic strength and the mole fraction of anionic surfactant (basis total surfactant). Nanoparticle formation was also reported by Thünemann et al. [10] in interactions between an amphoteric polyelectrolyte and an anionic surfactant. Nanoparticles in the size range 3–5 nm were formed at a molar ratio of 1:1 of the cationic group on the polymer and the anionic surfactant. The structure suggested was that of micelles coated by (“dressed by”) the ampholyte polymer.

In a previous paper [11] we showed that nanoparticles (35–150 nm) may be formed by interaction of an anionic surfactant, sodium dodecyl sulfate (SDS), with the cationic polyelectrolyte polydiallyldimethylammonium chloride (PDAC) in aqueous solution. Nanoparticles of various sizes and surface potentials having organized internal structure were obtained, depending on the SDS/PDAC molar ratio,  $r$  (referred to the PDAC monomeric charge unit). In the present paper we investigate SDS–PDAC nanoparticles by an atomic force microscope and study their solubilization ability by using hydrophobic probes, Nile Red (NIR), and pyrene. NIR (Fig. 1a) (9-(diethylamino)-5*H*-benzo[ $\alpha$ ]-phenoxazin-5-one) is a highly fluorescent, solvatochromic dye, in which the absorbance and emission maxima are

\* Corresponding author. Fax: +972 2 6584350.

E-mail address: [magdassi@cc.huji.ac.il](mailto:magdassi@cc.huji.ac.il) (S. Magdassi).

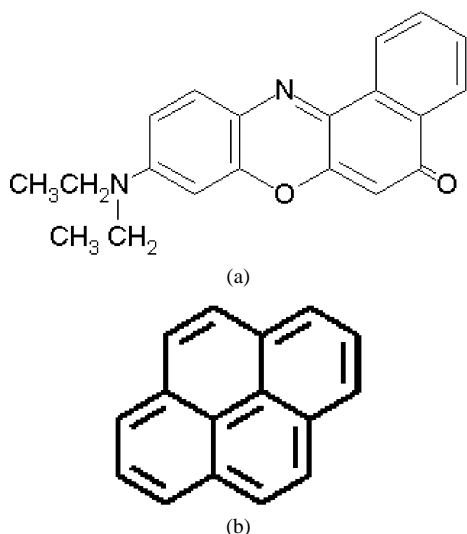


Fig. 1. Structure of Nile Red (a) and pyrene (b).

shifted to higher wavelengths with increasing polarity of the medium [12]. Nile Red is extensively applied to examine the structure, dynamics, and environment in biological and microheterogeneous systems, and was recently reported as a probe for microemulsions [13,14]. Therefore, NIR enables us to obtain information about its solubilization site in the nanoparticles.

Pyrene (Fig. 1b) shows interesting photophysical properties due to the long lifetime of its monomers and its efficient formation of excimers. Pyrene is one of the few condensed aromatic hydrocarbons, which shows significant fine structure (vibronic bands) in its monomer fluorescence spectra in solution. The vibrational fine structure intensities undergo significant perturbations on going from nonpolar solvents to polar solvents with high permanent dipoles. The five predominant peaks of pyrene are numbered I–V, and peak III shows maximum variations in intensity relative to peak I [15]. This 3/1 ratio will be used as an indication for the polarity of the environment in which the pyrene is solubilized, and also for determination of the critical association concentration, CAC, of SDS/PDAC systems.

## 2. Materials and methods

### 2.1. Materials

The following materials were used with no further purification: PDAC of molecular weight 100,000–200,000 g/mol, from Aldrich as a 21.8% (w/w) aqueous solution; SDS (minimum 98.5%, by gas chromatography) from Sigma; Nile Red from Fluka; and pyrene (minimum 97.5% by HPLC) from Aldrich.

Muscovite mica films were obtained from Pelco International and were freshly cleaved prior to spin coating.

### 2.2. Nanoparticle preparation and probes solubilization

SDS and PDAC stock solutions were prepared in deionized water, and SDS–PDAC particles were prepared as described in a previous paper [11]. Typically, 5 ml of SDS solution of the required concentration and 5 ml of PDAC solution (0.2% w/w) were poured simultaneously into a vial and were stirred immediately. Thus, the final PDAC concentration was kept constant, 0.1% w/w (6.8 mM, based on the monomer), in all experiments, while the SDS/PDAC molar ratio was varied.

In NIR solubilization experiments, the vials contained the hydrophobic probe, prior to the addition of the polymer and surfactant. The probe was placed in the vials as an ethanol solution in a volume of several microliters, depending on the required final concentration during the solubilization experiment. The ethanol was evaporated prior to the solubilization experiments. In pyrene solubilization experiments, pyrene was first dissolved in ethanol, and then a PDAC aqueous solution was prepared using a small portion of the pyrene solution after evaporation, according to the procedure of Kogej and Škerjanc [16]. The pyrene-containing PDAC solution was used to prepare SDS–PDAC samples by mixing with SDS solution. The pyrene concentration in all samples was  $1 \times 10^{-6}$  M. The samples were shaken for 48 h in a shaker at 25 °C, except the samples for the CMC evaluation, which were shaken for a week.

### 2.3. Ultrafiltration

Separation of the nanoparticles from the micelles was performed using Ultrafree microcentrifuge filters (Sigma) made of polysulfone membrane with 300 KD cutoff. Samples were twice centrifuged and resuspended with deionized water before absorbance or fluorescence spectra were measured.

### 2.4. Absorbance and fluorescence spectra

Absorbance spectra of the samples were taken using a Cary 100Bio spectrophotometer, a 1-cm polystyrene cell, and a scan rate of 600 nm/min.

Fluorescence spectra of samples were taken using a Cary Eclipse fluorimeter, a 1-cm quartz cell, and a scan rate of 1200 nm/min. In NIR experiments, excitation and emission slits were both fixed at 5 nm, and  $\lambda_{\text{ex}}$  was 500 nm. In the pyrene experiments the excitation and emission slits were fixed on 10 and 2.5 nm, respectively, and  $\lambda_{\text{ex}}$  was 335 nm.

### 2.5. Spin coating

A custom-made spinner was used for spin-coating experiments, which were carried out at room temperature. The sample was dispensed onto the central portion of the spinning surface (mica film for AFM imaging, and aluminum stub for SEM imaging), which was accelerated to a speed of

3100 rpm for 20 s. Upon cessation of spinning, the coated substrate was allowed to dry horizontally at 37 °C for 24 h before the AFM or SEM imaging was carried out.

## 2.6. Atomic force microscopy

Tapping mode imaging was carried out on a Solver P47 (NT-MDT, Moscow, Russia) scanning probe microscope. A 90- $\mu\text{m}$ -long Ultrasharp silicon tip coated with aluminum, with a radius of curvature of less than 10 nm (SC-12 series, NT-MDT), was used. This tip has a typical resonance frequency of 315 kHz and a typical force constant of 14.0 N/m. Height mode images were collected along with either amplitude or phase images. A scan rate of 0.45–1.2 Hz was typically sufficient to maintain a good signal-to-noise ratio. Multiple scans were performed in each case, with a variety of areas examined for consistent sample morphology. The AFM chamber was kept dry by using an open vial containing  $\text{CaCl}_2$  during and 1 h prior to imaging.

## 2.7. HR-SEM

Sirion HR-SEM with 1.5–2.5 nm point resolution was used to explore the SDS–PDAC particles. A drop of the sample was spin-coated on a stab, followed by coating with gold.

## 2.8. Light scattering

Size measurements were performed with a high-performance particle sizer (HPPS, Malvern Instruments). The SDS–PDAC sample, as aqueous dispersion, was measured without dilution. The calculation of size distribution from light scattering measurements is based on the assumption that the particles are spherical.

## 3. Results and discussion

### 3.1. Nanoparticle morphology

SEM image of SDS–PDAC nanoparticles prepared at SDS/PDAC charge molar ratio  $r = 0.3$  (refers to the PDAC monomeric charge unit) is presented in Fig. 2. During the drying of the dispersion of nanoparticles, a ring formation was observed. The images were taken from the outer part of the ring. As shown, the nanoparticles are aggregated, while each aggregate is composed of spherical particles having a diameter in the range 15–30 nm. By light-scattering measurements it was found that the average size is 17 nm (by number distribution).

AFM images of SDS–PDAC nanoparticles prepared at the same ratio as for the SEM imaging are seen in Figs. 3a and 3b, on wide and narrow fields, respectively. It appears that the particles have a spherical shape. It should be mentioned that the spin-coating process enabled viewing the particles without aggregation, compared to what was observed

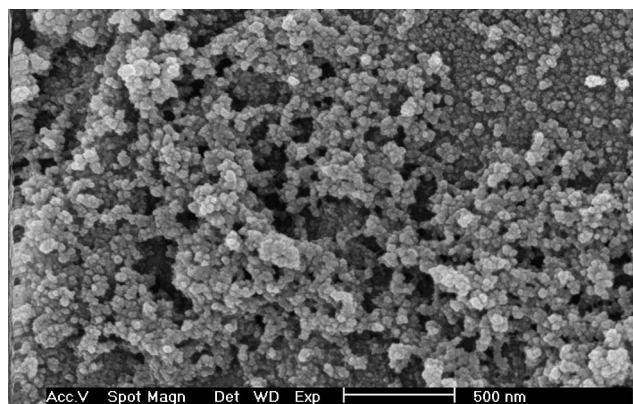


Fig. 2. HR-SEM image of SDS–PDAC nanoparticles prepared at  $r$  value of 0.3 (PDAC 6.8 mM, based on the monomeric unit, SDS  $2 \times 10^{-3}$  M).

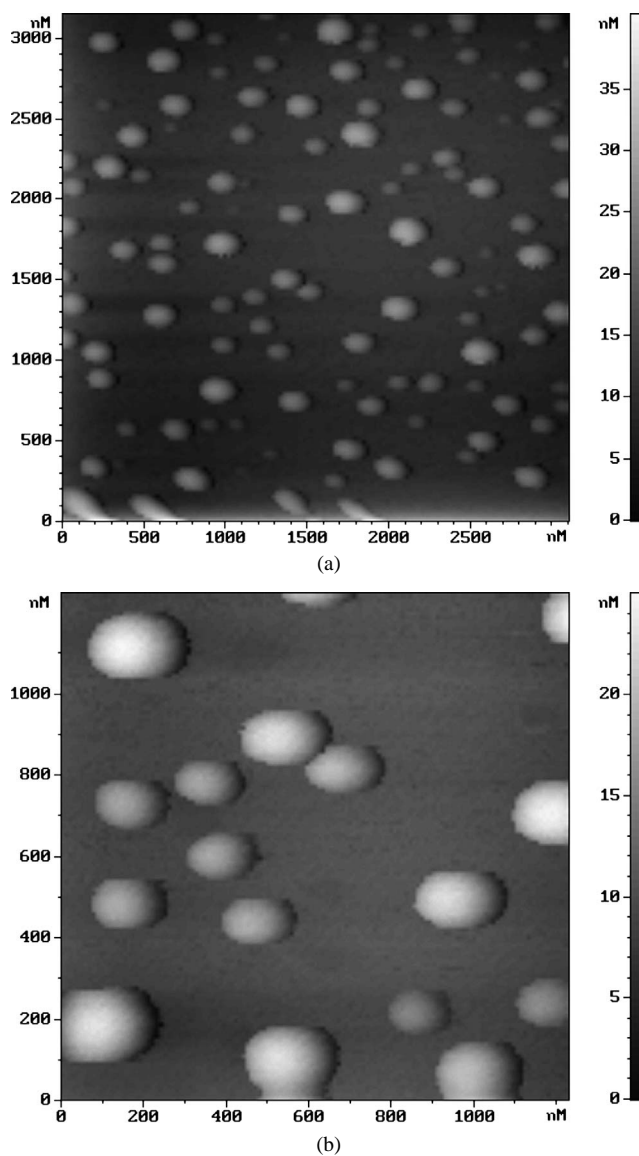


Fig. 3. AFM images of SDS–PDAC nanoparticles prepared at  $r$  value of 0.3 (PDAC 6.8 mM, based on the monomeric unit, SDS  $2 \times 10^{-3}$  M).

by the SEM. It should be mentioned that the exact size could not be determined by AFM due to tip convolution, which arises when the radius of curvature of the tip is comparable to, or greater than, the size of the feature to be imaged. In this case, as the tip scans over the specimen, the sides of the tip make contact before the apex, and the microscope begins to respond to the feature.

### 3.2. NIR solubilization

In order to evaluate the ability of SDS–PDAC nanoparticles to solubilize hydrophobic molecules, we first evaluated the solubilization of NIR in SDS micelles. From the fluorescence spectra of NIR in the SDS–water system presented in Fig. 4, it can be seen that SDS micelles indeed solubilize NIR, and that the fluorescence intensity increases with the increase in surfactant concentration (samples were filtered by 0.1  $\mu\text{m}$ ; thus nonsolubilized NIR was removed). From the absorbance intensity, it was found that the maximal ratio between NIR molecules and SDS micelles was about 1:4 (assuming SDS aggregation number of 60). The CMC value, which is obtained from the onset of increase in the fluorescence intensity curve (inset to Fig. 4), between  $6 \times 10^{-3}$  and  $8 \times 10^{-3}$  M SDS, is in good agreement with the literature value ( $8.16 \times 10^{-3}$  M at 25 °C) [17]. As reported, the NIR fluorescence lifetime markedly decreases with the increase in the hydrogen-bonding capability of the medium [18]. Therefore, the sudden rise in fluorescence intensity upon the formation of micelles results from the presence of NIR within the hydrophobic core of the micelles, being more protected from the water environment. It should be noted that there is a shift of  $\lambda_{\text{max}}$  toward longer wavelengths, from 617 up to 645 nm with the increase in SDS concentration. Since NIR is a solvatochromic dye, it was expected that the solubilization would cause an opposite shift due to the hydrophobic environment within the micelle, compared to water. A possible explanation is that below the CMC, the NIR molecules are aggregated in water, and their actual environment is hydrophobic. Evaluation of the fluorescence of a dispersion of NIR particles in water, indicates that the peak

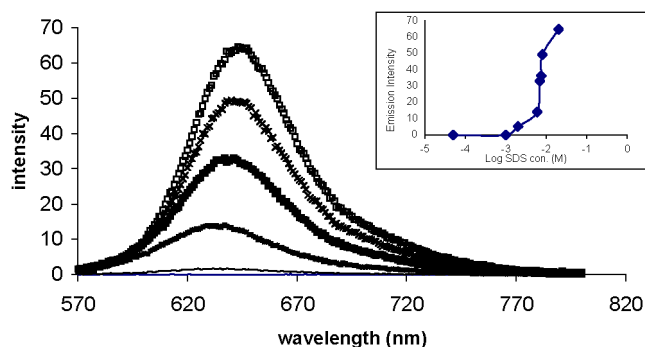


Fig. 4. Emission spectra of NIR in SDS solutions at various concentrations:  $5 \times 10^{-3}$  M (—),  $6 \times 10^{-3}$  M (···),  $7 \times 10^{-3}$  M (■),  $8 \times 10^{-3}$  M (×),  $2 \times 10^{-2}$  M (□),  $\lambda_{\text{ex}} = 500$  nm. Inset: Emission intensity of NIR as a function of SDS concentration.

is at 589 nm, indicating again a very hydrophobic environment.

At the next stage, we evaluated the possibility of direct solubilization of NIR within the SDS–PDAC nanoparticles, which were prepared at various charge ratios. As shown in Fig. 5, while particles were prepared at low ratio,  $r = 0.52$ , in which we assume that there are no free SDS micelles, NIR is indeed solubilized, having an emission peak at 634 nm compared to 645 nm for micelles. At higher  $r$  values, such as 5 and 10, the emission peak of NIR is the same as in the SDS micelles (Fig. 6), 644 nm. At these high  $r$  values, there should be a mixture of nanoparticles and free micelles. Therefore, the micelles were separated from the nanoparticles by ultrafiltration (From preliminary experiments regarding ultrafiltration of micelles it was found that 300 KD cutoff membranes allows the migration of free micelles.) It was found that after ultrafiltration of these samples and resuspension of the nanoparticles, the emission peak is obtained again at 634 nm, as in the nanoparticles prepared at low  $r$  value (Fig. 6). Therefore, it should be concluded that at high  $r$  ratios both micelles and SDS–PDAC nanoparticles exist in solution, while both solubilize the hydrophobic molecule.

Similar phenomena of peak shift are seen also for the absorbance spectra of the same samples, while the “nanoparticle peak” is at 560 nm and the “micelle peak” is at 575 nm. It is interesting to note that the absorbance of a nanoparticle peak is similar to the peak obtained for NIR in an 80/20

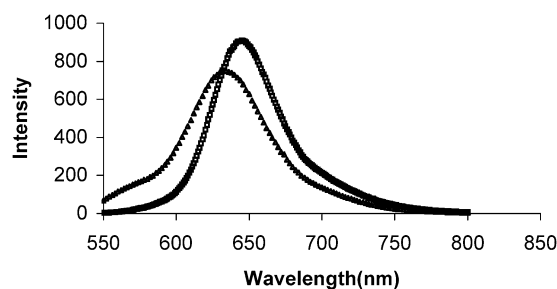


Fig. 5. Emission spectra of NIR in SDS micelles (□) and in SDS–PDAC particles prepared at  $r = 0.52$  (Δ),  $\lambda_{\text{ex}} = 500$  nm.

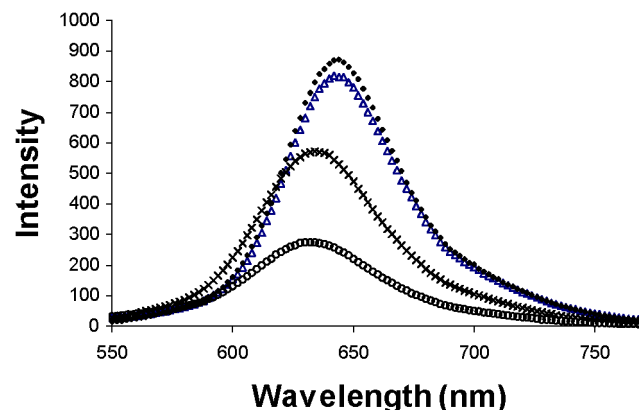


Fig. 6. Emission spectra of NIR in SDS–PDAC samples at  $r$  value 5 (Δ) and 10 (◆) and the same samples after ultrafiltration,  $r = 5$  (○) and  $r = 10$  (×),  $\lambda_{\text{ex}} = 500$  nm.

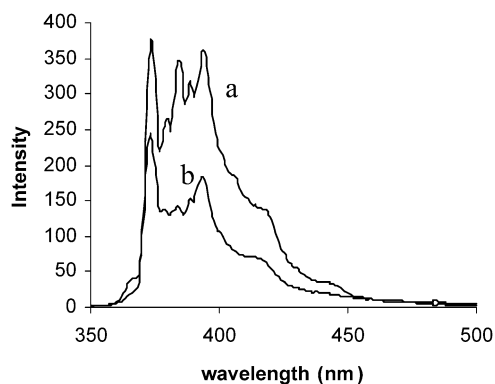


Fig. 7. Emission spectra of pyrene in SDS micelles (a) and in SDS-PDAC nanoparticles (b),  $\lambda_{\text{ex}} = 335$  nm.

ethanol/water mixture, as reported by Deye et al. [19]. This indicates that NIR is not solubilized within a micelle-like environment (absorbance peak at 575 nm), but rather in a new environment, which is more hydrophobic. These results also indicate that the NIR is not solubilized within the internal core of micelle.

It should be emphasized that the pH measured in all experiments was above 6.5, while the  $pK_a$  of NIR [20] is between 6 and 7. It was found that at pH higher than 6.5 there is no change in emission intensity peak wavelength. However, acidifying the samples (pH  $\sim 3$ ) results in a great shift of the emission peak to 675 nm, which is in any case higher than that observed during the solubilization experiments. NIR solubilized in SDS micellar solution at pH 3 also yields a peak at 675 nm.

### 3.3. Pyrene in SDS/PDAC nanoparticles

As reported by Kogej and Škerjanc [16], pyrene may be used to evaluate aggregate formation according to the  $I_1/I_3$  ratio of the fluorescence spectra.

Fig. 7 presents typical fluorescence spectra for pyrene in SDS micelles and in SDS/PDAC nanoparticles. From such curves, the  $I_1/I_3$  values are calculated for series of samples prepared at various SDS concentrations and shown in Fig. 8, as a function of log SDS concentration. From Fig. 7 it can also be seen that no pyrene excimer peak exists in the spectra (should be seen at  $\sim 470$  nm). The pyrene concentration in all experiments is very low ( $1 \times 10^{-6}$  M), and based on reports regarding pyrene in hexane solutions [21] or in micelles [22], pyrene excimer does not form at such concentrations.

At the first part of the curve in Fig. 8,  $I_1/I_3$  is almost constant, 1.7, and has a value typical for aqueous solutions [23,24]. A solution of pyrene in PDAC without a surfactant shows a similar ratio, 1.69.

At higher SDS concentrations  $I_1/I_3$  starts to decrease due to solubilization of pyrene in the hydrophobic domains formed by the polymer-surfactant complexes. From the first break in this curve, the CAC can be determined [25,26]. In our system, the CAC is  $5 \times 10^{-6}$  M SDS, which is about three orders of magnitudes below the CMC, due to the strong

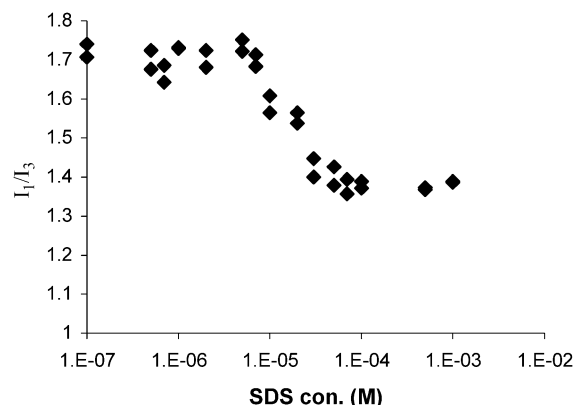


Fig. 8. Duplicate  $I_1/I_3$  ratios of pyrene in the presence of SDS-PDAC particles, at various SDS concentrations. PDAC concentration is fixed, 0.1% (6.8 mM, based on the monomer);  $\lambda_{\text{ex}} = 335$  nm.

electrostatic attraction between the polyelectrolyte and the surfactant. A similar ratio between CMC to CAC,  $\sim 1800$ , was also observed by Kogej and Škerjanc [16], for the interaction between dodecyltrimethylammonium bromide and poly(styrenesulfonate). It is interesting to note that above the CAC, the  $I_1/I_3$  ratio reaches a constant value, about 1.3–1.4, indicating constant polarity of the local environment sensed by pyrene, as also observed by Kogej and Škerjanc [16], and interpreted as micelle-like aggregation of surfactants in the presence of the polycation. However, this value is higher than the value obtained for solubilization within SDS micelles (about 1.1) [24]. This indicates that pyrene is solubilized within the polymer-surfactant nanoparticles in an environment that is more polar than in the micelle core, as opposed to solubilization of Nile Red.

General and Thünemann [27] used pyrene to evaluate the ability of nanoparticles to release hydrophobic compounds while triggered by pH change. In their complexes (composed of polyaminoacid-dodecanoate), the  $I_1/I_3$  was used as an indication of whether the hydrophobic probe is within the complexes or in the aqueous phase.

## 4. Summary

Association between PDAC and SDS starts at very low SDS concentrations was revealed by pyrene fluorescence experiments. The nanoparticles formed can solubilize hydrophobic molecules spontaneously, while the solubilization site in the nanoparticles differs from the site in SDS micelles. Pyrene shows a more polar vicinity in the particles compared to that in the micelles, but a more hydrophobic environment compared to PDAC itself. NIR is solubilized at a more hydrophobic domain in the nanoparticles, compared to SDS micelles. The differences in solubilization of pyrene and NIR are most probably due to their different chemical structures.

It is expected that the findings regarding solubilization within SDS-PDAC nanoparticles would lead to utilization

of such particles as delivery systems for hydrophobic molecules in the pharmaceuticals and cosmetic industries. Obviously, in these applications additional issues such toxicological information should be taken into consideration.

### Acknowledgments

This work was supported in part by grants from the European Union NACBO program and from the Israel Ministry of Industry and Commerce, NFM MAGNET program.

### References

- [1] F. Winnik, S.T.A. Regismond, L. Picullel, B. Lindman, G. Karlstrom, R. Zana, in: J.C.T. Kwak (Ed.), *Polymer–Surfactant Systems*, vol. 77, Dekker, New York, 1998, pp. 65–142, 267–316, 409–454.
- [2] E.D. Goddard, K.P. Ananthapandmanabhan, in: *Interactions of Surfactants with Polymers and Proteins*, CRC Press, Boca Raton, FL, 1993.
- [3] B. Cabane, R. Duplessix, *Colloids Surf.* 13 (1985) 19.
- [4] J.C. Brackman, J.B.F.N. Engberts, *J. Colloid Interface Sci.* 132 (1989) 250.
- [5] J.C. Brackman, J.B.F.N. Engberts, *Langmuir* 7 (1991) 2097.
- [6] E.D. Goddard, *Colloids Surf.* 19 (1986) 301.
- [7] B. Lindman, K. Thalberg, in: E.D. Goddard, K.P. Ananthapandmanabhan (Eds.), *Polymer–Surfactant Interactions*, CRC Press, Boca Raton, FL, 1993, p. 203.
- [8] A.F. Thünemann, *Prog. Polym. Sci.* 27 (2002) 1473.
- [9] P.L. Dubin, R. Oteri, *J. Colloid Interface Sci.* 95 (1983) 453.
- [10] A.F. Thünemann, K. Sander, W. Jaeger, R. Dimova, *Langmuir* 18 (2002) 5099.
- [11] G. Nizri, S. Magdassi, J. Schmidt, Y. Cohen, Y. Talmon, *Langmuir* 20 (2004) 4380.
- [12] A. Datta, D. Mandal, S. Kumar Pal, K. Bhattacharyya, *J. Phys. Chem. B* 101 (1997) 10,221.
- [13] M.E.C.D.R. Oliveira, G. Hungerford, M. da G. Miguel, H.D. Burrows, *J. Mol. Struct.* 563–564 (2001) 443.
- [14] M. Ben Moshe, S. Magdassi, Y. Cohen, L. Avram, *J. Colloid Interface Sci.* 276 (2004) 221.
- [15] K. Kalyanasundaram, J.K. Thomas, *J. Am. Chem. Soc.* 99 (1977) 2039.
- [16] K. Kogej, J. Škerjanc, *Langmuir* 15 (1999) 4251.
- [17] B.D. Flockhart, *J. Colloid Sci.* 16 (1961) 484.
- [18] A. Cser, K. Nagy, L. Biczok, *Chem. Phys. Lett.* 360 (2002) 47.
- [19] J.F. Deye, T.A. Berger, A.G. Anderson, *Anal. Chem.* 62 (1990) 615.
- [20] Z. Stransky, V. Stuzka, *Chem. Zvesti* 22 (1968) 341.
- [21] D.A. Van Dyke, B.A. Pryor, P.G. Smith, M.R. Topp, *J. Chem. Ed.* 75 (1998) 615.
- [22] C. Honda, M. Itagaki, R. Takeda, K. Endo, *Langmuir* 18 (2002) 1999.
- [23] F.M. Winnik, S.T.A. Regismond, *Colloids Surf. A* 118 (1996) 1.
- [24] D.S. Karpovich, G.J. Blanchard, *J. Phys. Chem.* 99 (1995) 3951.
- [25] P. Hansson, M. Almgren, *Langmuir* 10 (1994) 2115.
- [26] P. Hansson, M. Almgren, *J. Phys. Chem.* 99 (1995) 16684.
- [27] S. General, A.F. Thünemann, *Int. J. Pharm.* 230 (2001) 11.